

Supporting Information

Graphene-Assisted Synergistic Electronic DOS Modulation and Phonon Scattering to Improve the Thermoelectric Performance of Mg₃Sb₂-Based Materials

*Qiang Zhang,^{*abc} Jiadang Li,^a Nagendra S. Chauhan,^c Lifei Wang,^{be} Zhicheng Huang,^c Wenhao Fan,^d Kei Hayashi,^c Shaoping Chen,^e Jianfeng Fan,^{ab} Yuzuru Miyazaki^c*

a. Key Laboratory of Interface Science and Engineering in Advanced Materials, Ministry of Education, Taiyuan University of Technology, Taiyuan 030024, China

b. Shanxi Key Laboratory of Advanced Magnesium-Based Materials, Taiyuan University of Technology, Taiyuan 030024, China

c. Department of Applied Physics, Graduate School of Engineering, Tohoku University, Sendai 980-8579, Japan

d. College of Physics and Optoelectronics, Taiyuan University of Technology, Taiyuan 030024, China

e. College of Materials Science and Engineering, Taiyuan University of Technology, Taiyuan 030024, China

*Correspondence should be addressed to Qiang Zhang: zhangqiang@tyut.edu.cn

1 Experimental section and theoretical calculation

First-principles calculations

Some basic information regarding the first-principles calculations is given below: **Tabs.1-4** and **Figs. 1-4.**

Tabs. 1 Parameters of Mg₃Sb₂ and graphene crystal structure

Items	Structure parameter
	Space group P-3m1 (No. 164)
Mg ₃ Sb ₂	Lattice constant (Å) a=b=4.55 c=7.24 $\alpha=\beta=90.000^\circ, \gamma=120.000^\circ$
Mg (I)	(0, 0, 0)
Mg (II)	(0.3333, 0.6667, 0.3669)
Sb	(0.3333, 0.6667, 0.7738)
	Space group P6mm
Graphene	Lattice constant (Å) a=b=7.38 $\gamma=120.000^\circ$
C (I)	(0.3333, 0.6667, 0)
C (II)	(0.6667, 0.3333, 0)

Tabs. 2 Parameters of geometrical optimization

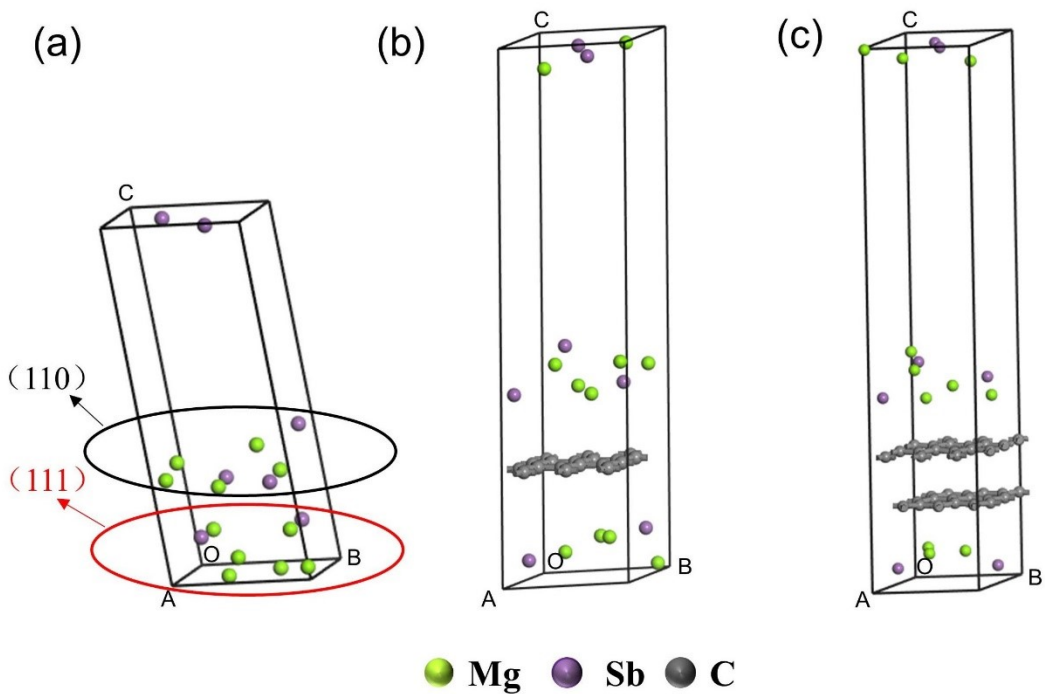
Items	Parameters
Functional	GGA-PBE
Plane-wave cutoff energy	400 eV
Self-consistent field	Fine 1×10^{-5} eV/atom
Monkhorst-Pack <i>k</i> -point mesh	$1\times1\times1$
Pseudopotential	norm-conserving

Tabs. 3 Parameters of calculation for energy band structure

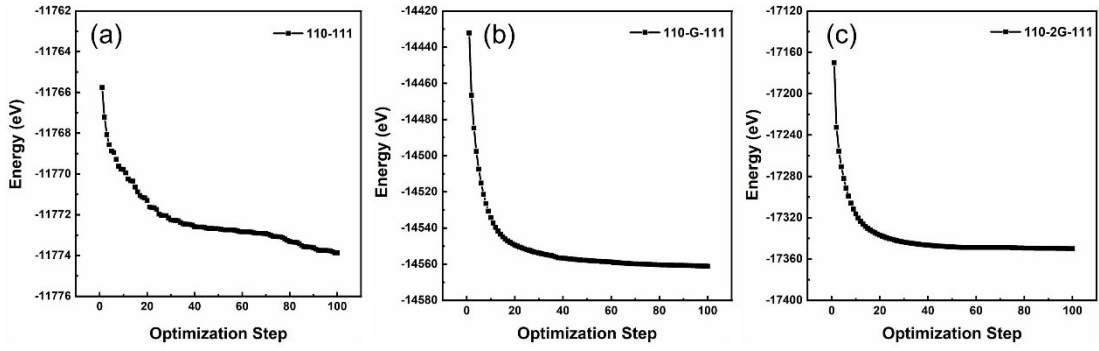
Items	Parameters
Functional	GGA-PBE
Interval	0.015/Å
High symmetry points	Γ , K, H, A
Path	Γ -K-H-A- Γ

Tabs. 4 Parameters of calculation for density of states

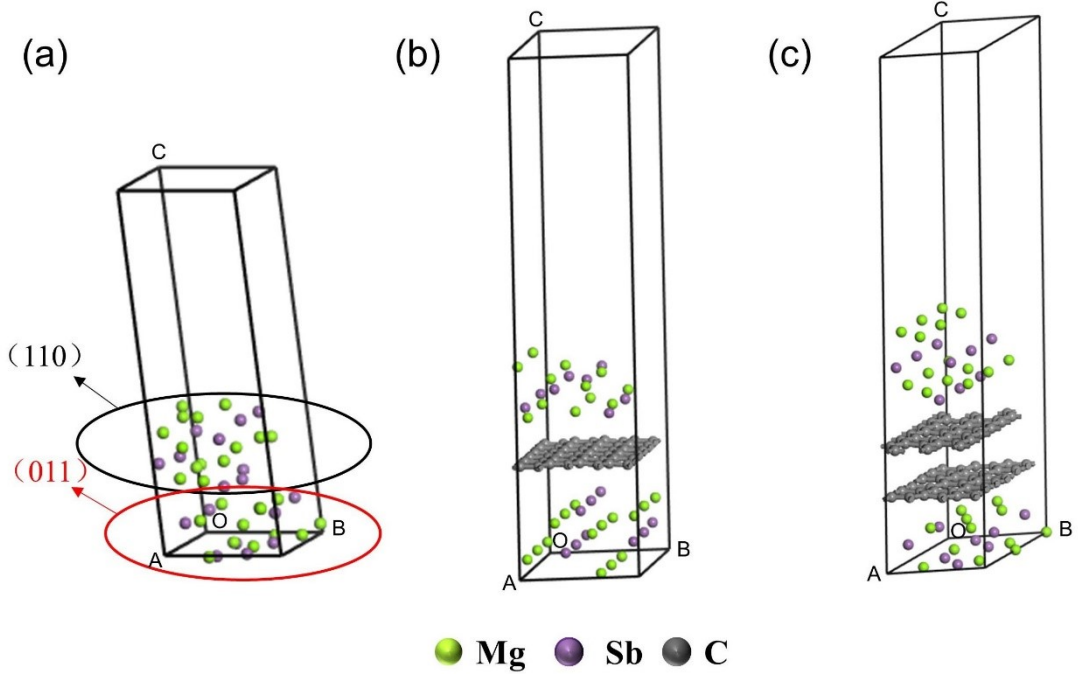
Item	Parameters
Functional	GGA-PBE
k -point mesh	8x8x8



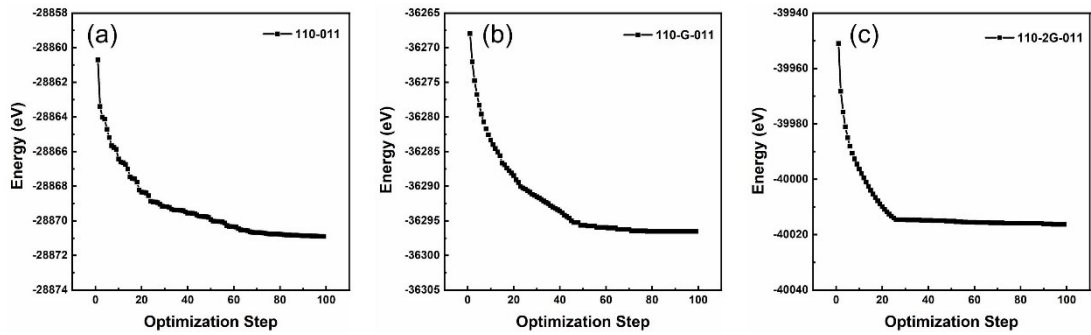
Figs. 1 Unit cell of three interface structures: (a) $\text{Mg}_3\text{Sb}_2(110)|\text{Mg}_3\text{Sb}_2(111)$, (b) $\text{Mg}_3\text{Sb}_2(110)|\text{G}(1\text{layer})|\text{Mg}_3\text{Sb}_2(111)$, (c) $\text{Mg}_3\text{Sb}_2(110)|\text{G}(2\text{layers})|\text{Mg}_3\text{Sb}_2(111)$.



Figs. 2 Geometry optimization processes for the three interface structures: (a) Mg₃Sb₂(110)|Mg₃Sb₂(111), (b) Mg₃Sb₂(110)|G(1layer)|Mg₃Sb₂(111), (c) Mg₃Sb₂(110)|G(2layers)|Mg₃Sb₂(111).



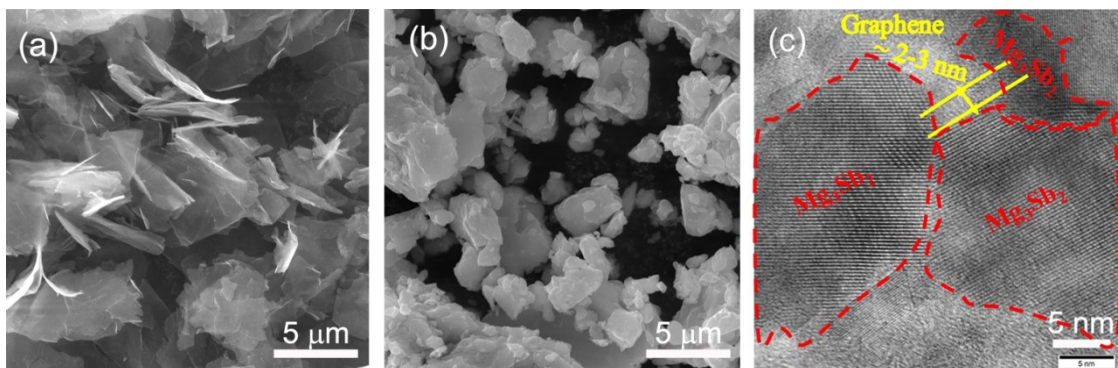
Figs. 3 Unit cell of three interface structures: (a) Mg₃Sb₂(110)|Mg₃Sb₂(011), (b) Mg₃Sb₂(110)|G(1layer)|Mg₃Sb₂(011), (c) Mg₃Sb₂(110)|G(2layers)|Mg₃Sb₂(011).



Figs. 4 Geometry optimization processes for the three interface structures: (a) $\text{Mg}_3\text{Sb}_2(110)|\text{Mg}_3\text{Sb}_2(011)$, (b) $\text{Mg}_3\text{Sb}_2(110)|\text{G}(1\text{layer})|\text{Mg}_3\text{Sb}_2(011)$, (c) $\text{Mg}_3\text{Sb}_2(110)|\text{G}(2\text{layers})|\text{Mg}_3\text{Sb}_2(011)$.

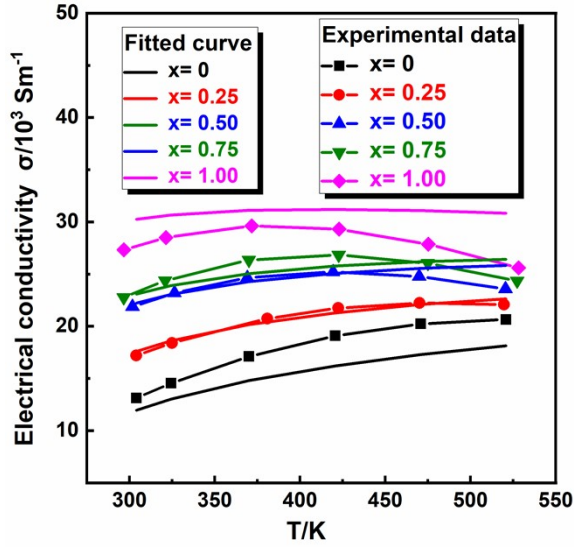
2 Results and Discussion

2.1 Phase composition and microstructure characterization



Figs. 5 (a) 2-dimensional graphene raw materials; (b) morphology of BM-ed powders of $\text{Mg}_{3.24}\text{Sb}_{1.5}\text{Bi}_{0.49}\text{Te}_{0.01}/1.0$ vol% G; (c) TEM photos of grain boundary graphene for the $\text{Mg}_{3.24}\text{Sb}_{1.5}\text{Bi}_{0.49}\text{Te}_{0.01}/1.0$ vol% G sample.

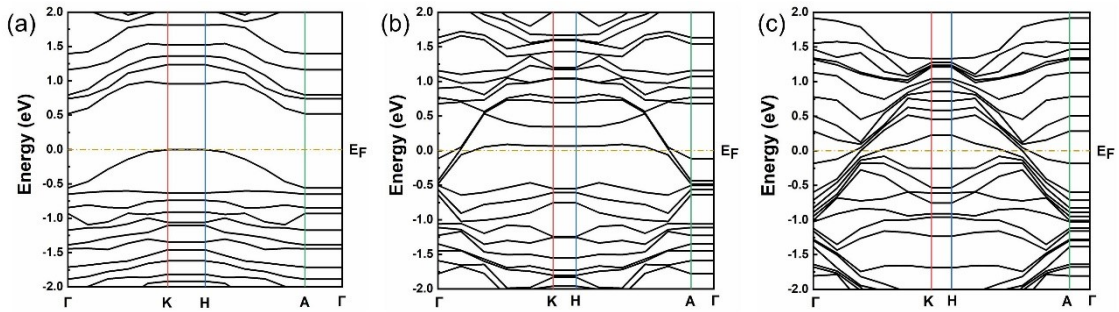
2.2 Electrical transport properties of $\text{Mg}_{3.24}\text{Sb}_{1.5}\text{Bi}_{0.49}\text{Te}_{0.01}/x$ vol% G ($x=0-1.25$) samples



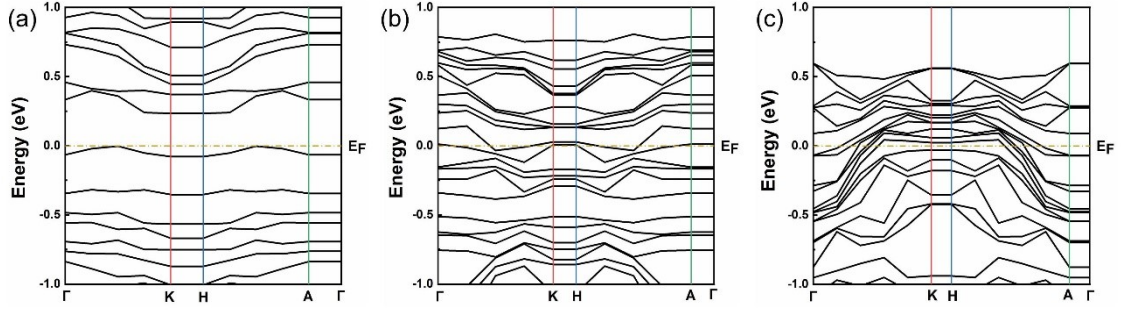
Figs. 6 The corresponding fitted curves and experimental data based on the trapping state model.

Tabs. 5 The parameters used for fitted curves based on the trapping state model.

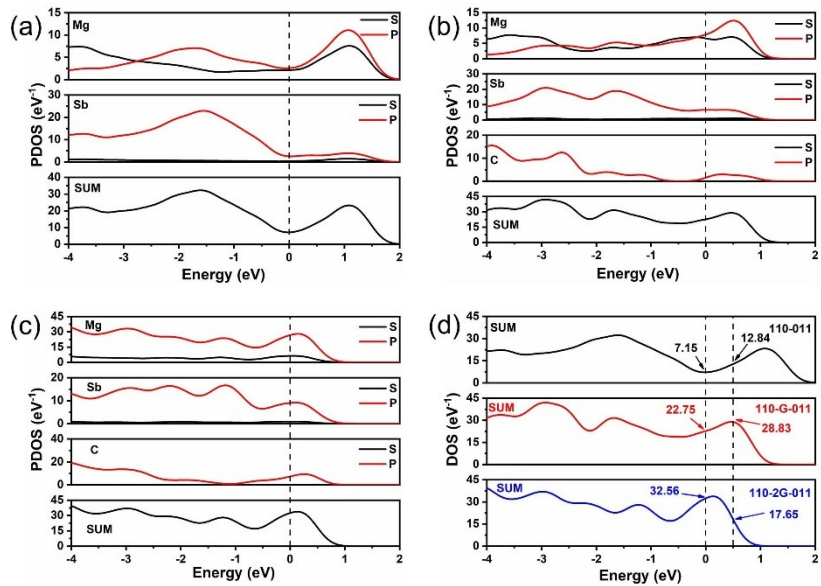
Sample	Temperatur e range /K	Elementary charge e/C	Grain size d/m	Carrier density n/m ⁻³	Effective mass m*	Boltzmann constant k _B /JK ⁻¹	Barrier height E _b /meV
x=0	300-525	1.60×10 ⁻¹⁹	2.0×10 ⁻⁶	2.0×10 ²⁵	1.2 m _e	1.38×10 ⁻²³	42
x=0.25	300-525	1.60×10 ⁻¹⁹	2.0×10 ⁻⁶	2.0×10 ²⁵	1.2 m _e	1.38×10 ⁻²³	32
x=0.5	300-525	1.60×10 ⁻¹⁹	2.0×10 ⁻⁶	2.0×10 ²⁵	1.2 m _e	1.38×10 ⁻²³	25
x=0.75	300-525	1.60×10 ⁻¹⁹	2.0×10 ⁻⁶	2.0×10 ²⁵	1.2 m _e	1.38×10 ⁻²³	26
x=1.0	300-525	1.60×10 ⁻¹⁹	2.0×10 ⁻⁶	2.0×10 ²⁵	1.2 m _e	1.38×10 ⁻²³	18



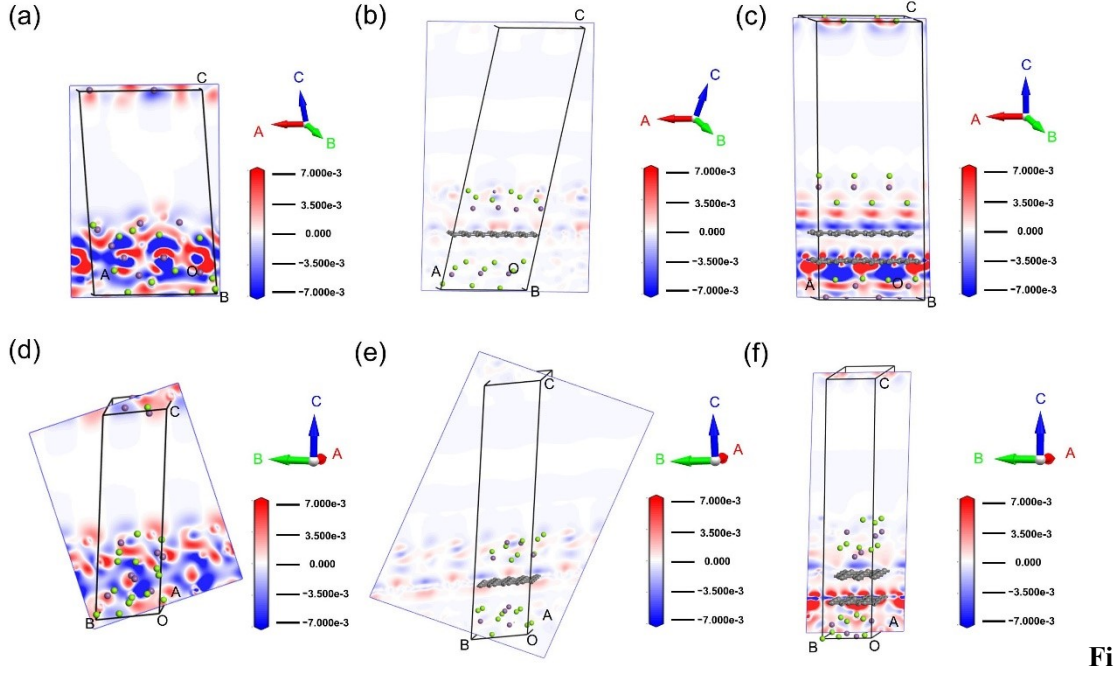
Figs. 7 Energy band structures of the three interface structures: (a) Mg₃Sb₂(110)|Mg₃Sb₂(111), (b) Mg₃Sb₂(110)|G(1layer)|Mg₃Sb₂(111), (c) Mg₃Sb₂(110)|G(2layers)|Mg₃Sb₂(111).



Figs. 8 Energy band structures of the three interface structures: (a) $\text{Mg}_3\text{Sb}_2(110)|\text{Mg}_3\text{Sb}_2(011)$, (b) $\text{Mg}_3\text{Sb}_2(110)|\text{G}(1\text{layer})|\text{Mg}_3\text{Sb}_2(011)$, (c) $\text{Mg}_3\text{Sb}_2(110)|\text{G}(2\text{layers})|\text{Mg}_3\text{Sb}_2(011)$.



Figs. 9 Electronic DOS of three interface structures: (a) $\text{Mg}_3\text{Sb}_2(110)|\text{Mg}_3\text{Sb}_2(111)$, (b) $\text{Mg}_3\text{Sb}_2(110)|\text{G}(1\text{layer})|\text{Mg}_3\text{Sb}_2(111)$, (c) $\text{Mg}_3\text{Sb}_2(110)|\text{G}(2\text{layers})|\text{Mg}_3\text{Sb}_2(111)$ and (d) the contrast of the total DOS of the three interface structures.



Fi

gs. 10 Charge density difference maps of three interface structures: (a), (d) $\text{Mg}_3\text{Sb}_2(110)|\text{Mg}_3\text{Sb}_2(011)$; (b), (e) $\text{Mg}_3\text{Sb}_2(110)|\text{G}(1\text{layer})|\text{Mg}_3\text{Sb}_2(011)$; (c), (f) $\text{Mg}_3\text{Sb}_2(110)|\text{G}(2\text{layers})|\text{Mg}_3\text{Sb}_2(011)$ with (a),(b), (c)//(A,C) plane and (d), (e), (f)//(B,C) plane.

2.3 Thermal transport properties of $\text{Mg}_{3.24}\text{Sb}_{1.5}\text{Bi}_{0.49}\text{Te}_{0.01}/x \text{ vol\% G}$ ($x=0-1.25$) samples

To illustrate the effects of G on phonon scattering processes, we employed the Debye-Callaway model to quantitatively differentiate the respective contributions from different phonon scattering mechanisms, and the related equations are given below¹⁻³:

$$\kappa_L = \frac{4\pi k_B}{v_s} \left(\frac{k_B T}{h}\right)^3 \int_0^{\theta_D/T} \tau_{tot} \frac{y^4 e^y}{(e^y - 1)^2} dy \quad (1)$$

$$\tau_{tot}^{-1} = \tau_B^{-1} + \tau_{PD}^{-1} + \tau_U^{-1} + \tau_{NP}^{-1} \quad (2)$$

$$\tau_B^{-1} = \frac{v_s}{d_{avg}} \quad (3)$$

$$\tau_{PD}^{-1} = A \omega^4 = \frac{\bar{V} \Gamma}{4\pi v_s^3} \omega^4 \quad (4)$$

$$\tau_U^{-1} = B\omega^2 T \exp\left(-\frac{\theta_D}{3T}\right) = \frac{h\gamma^2}{2\pi M_{avg} v_s^2 \theta_D} \omega^2 T \exp\left(-\frac{\theta_D}{3T}\right)$$

(5)

$$\tau_{NP}^{-1} = v_s V_{NP} \left[(2\pi R^2)^{-1} + \left(\frac{4}{9} \pi R^2 (\Delta\rho/\rho_0)^2 (\omega R/v_s)^4 \right)^{-1} \right]^{-1} \quad (6)$$

$$\theta_D = \frac{h}{k_B} \left(\frac{3N}{4\pi V} \right)^{1/3} v_s \quad (7)$$

$$\Gamma = \Gamma_m + \Gamma_s \quad (8)$$

$$\Gamma_m = \frac{\sum_{i=1}^n c_i \left(\frac{\bar{M}}{M} \right)^2 f_1 f_2 \left(\frac{M_1 - M_2}{M} \right)^2}{\sum_{i=1}^n c_i} \quad (9)$$

$$\Gamma_s = \frac{\sum_{i=1}^n c_i \left(\frac{\bar{M}}{M} \right)^2 f_1 f_2 \varepsilon \left(\frac{r_1 - r_2}{\bar{r}} \right)^2}{\sum_{i=1}^n c_i} \quad (10)$$

$$M = f_1 M_1 + f_2 M_2 \quad (11)$$

$$\bar{M} = \left(\frac{\sum_{i=1}^n c_i \bar{M}}{\sum_{i=1}^n c_i} \right) \quad (12)$$

$$\bar{r} = f_1 r_1 + f_2 r_2 \quad (13)$$

$$\varepsilon = \frac{2}{9} \left(\frac{6.4 \times \gamma (1 + \nu)}{1 - \nu} \right)^2$$

(14)

Where $y = \hbar\omega/k_B T$, τ , d_{avg} , θ_D , \bar{V} , γ , N , \hbar , ω , ν , ε are the reduced phonon energy, the phonon relaxation

time, the average grain size, the Debye temperature, the average atomic volume, the Grüneisen parameter, and the number of atoms in a primitive unit cell, the reduced Planck constant, the phonon frequency, Poisson's ratio, strain field-related adjustable parameter, respectively.

Tabs. 6 Parameters related to the Debye-Callaway model calculation

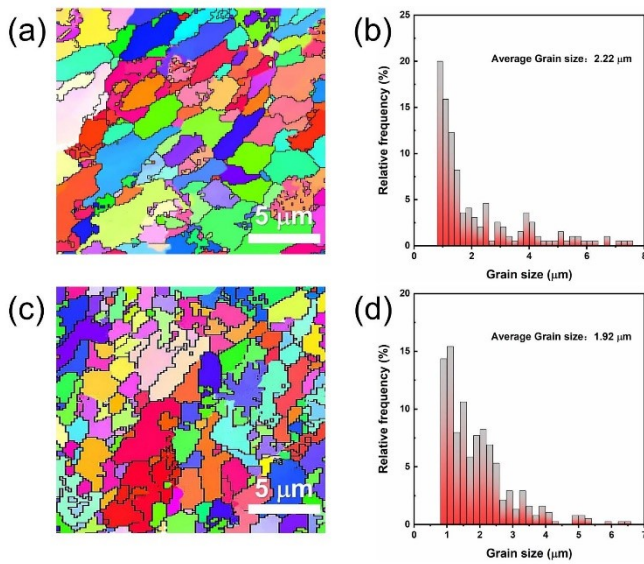
Parameters	Symbol	Value
Average sound velocity	v_s	2155 ms ⁻¹ [4]
Debye temperature	θ_D	215 K [5]
Debye frequency	ω_D	2.81×10^{13} s ⁻¹ [Cal. from θ_D]
Grüneisen parameter	γ	1.87 [6]
Poisson's ratio	ν	0.34 [5]
Average atomic mass	\bar{M}	1.20×10^{-25} kg [Cal.]
Average atomic volume	\bar{V}	2.62×10^{-29} m ³ [Cal.] 2.20 μm [Cal.]
Average grain size	d_{avg}	2.22 μm [Exp.] (Figs. 11(a), (b)) 1.92 μm [Exp.] (Figs. 11(c), (d))
Density of graphene	ρ_G	2.20×10^3 kgm ⁻³ [7]
Density of matrix	ρ	4.40×10^3 kgm ⁻³ [Exp.]
Mass fluctuation parameter	Γ_m	0.110 [Cal.]
Strain fluctuation parameter	Γ_s	0.426 [Cal.]
strain field-related adjustable parameter	ε	134.21 [Cal.]
Point-defect phonon scattering factor	A	1.15×10^{-40} s ³ [Cal.]
U-process phonon scattering factor	B	3.08×10^{-18} sK ⁻¹ [Cal.] 68 nm (x=0.25) 69 nm (x=0.50) 75 nm (x=0.75) 89 nm (x=0.10)
Equivalent size	R	6.05 × 10 ¹⁸ m ⁻³ (x=0.25) 1.21 × 10 ¹⁹ m ⁻³ (x=0.50) 1.81 × 10 ¹⁹ m ⁻³ (x=0.75) 2.42 × 10 ¹⁹ m ⁻³ (x=0.10) [Cal.]
Number density of graphene	V_{NP}	

Footnote: (1) [No.] -From reference; (2) [Cal.] -From calculation; (3) [Exp.] -From experiment.

Tabs. 7 τ_{tot}^{-1} in κ_s as a function of the reduced phonon energy y

Sample	τ_B^{-1} (s ⁻¹)	τ_{PD}^{-1} (s ⁻¹)	τ_U^{-1} (s ⁻¹)	τ_{NP}^{-1} (s ⁻¹)
x=0	9.80×10^8	$2.74 \times 10^{14} y^4$	$1.12 \times 10^{12} y^2$	--
x=0.25	9.80×10^8	$2.74 \times 10^{14} y^4$	$1.12 \times 10^{12} y^2$	$1.30 \times 10^{22} / (3.44 \times 10^{13} + 262 y^4)$
x=0.50	9.80×10^8	$2.74 \times 10^{14} y^4$	$1.12 \times 10^{12} y^2$	$2.61 \times 10^{22} / (3.34 \times 10^{13} + 240 y^4)$
x=0.75	9.80×10^8	$2.74 \times 10^{14} y^4$	$1.12 \times 10^{12} y^2$	$3.90 \times 10^{22} / (2.83 \times 10^{13} + 146 y^4)$

x=1.0	9.80×10^8	$2.74 \times 10^{14} \text{ y}^4$	$1.12 \times 10^{12} \text{ y}^2$	$5.22 \times 10^{22} / (2.01 \times 10^{13} + 52.3 \text{ y}^{-4})$
-------	--------------------	-----------------------------------	-----------------------------------	---



Figs. 11 $\text{Mg}_{3.24}\text{Sb}_{1.5}\text{Bi}_{0.49}\text{Te}_{0.01}/0$ vol% G (a) EBSD map, (b) grain size ; $\text{Mg}_{3.24}\text{Sb}_{1.5}\text{Bi}_{0.49}\text{Te}_{0.01}/1.0$ vol% G (c) EBSD map, (d) grain size

References:

1. J. Callaway and H. C. von Baeyer, *Physical Review*, 1960, **120**, 1149.
2. J. He, S. N. Girard, M. G. Kanatzidis and V. P. Dravid, *Advanced Functional Materials*, 2010, **20**, 764-772.
3. D. An, S. Chen, Z. Lu, R. Li, W. Chen, W. Fan, W. Wang and Y. Wu, *ACS applied materials & interfaces*, 2019, **11**, 27788-27797.
4. B. Zhu, X. Lu, J. Li, W. Xie, L. Wang, Q. Zhang, J. Fan and Y. Zheng, *ChemNanoMat*, 2023, **9**, e202200400.
5. M. T. Agne, K. Imasato, S. Anand, K. Lee, S. K. Bux, A. Zevalkink, A. J. Rettie, D. Y. Chung, M. G. Kanatzidis and G. J. Snyder, *Materials Today Physics*, 2018, **6**, 83-88.
6. J. Li, S. Zhang, B. Wang, S. Liu, L. Yue, G. Lu and S. Zheng, *Journal of Materials Chemistry A*, 2018, **6**, 20454-20462.
7. D. Chung, *Journal of materials science*, 2002, **37**, 1475-1489.